FLOOR ACCELERATION AMPLIFICATION ANALYSIS OF INSTRUMENTED BUILDING STRUCTURES

B. Huang [1], X. Hua [2], S. Günay [3], W. Lu [4]

[1] *Associate Professor, College of Civil Engineering, Nanjing Tech University, Nanjing China. baofeng@njtch.edu.cn*
[2] *Graduate Student, College of Civil Engineering, Nanjing Tech University, Nanjing China. huaxia2017nj@njtech.edu.cn*
[3] *Project Scientist, Pacific Earthquake Engineering Research Centre, Berkeley CA USA. selimgunay@berkeley.edu*
[4] *Professor, College of Civil Engineering, Tongji University, Shanghai China, wally@tongji.edu.cn*

Abstract

In seismic design of the acceleration sensitive nonstructural components and their anchors, such as the floor mounted equipment, ceiling, curtain wall, etc., floor acceleration amplification (FAA) factor is one of the most important parameters, representing the amplification of ground motion along the height of the main building structure. Generally, the maximum acceleration profile along the height of the building depends on the structural type, configuration, height, type, amplitude and frequency contents of the ground motion, etc., The complicated dependence of FAA on many variables may make it difficult to develop a representative distribution or simplified computation method to be used for seismic design. In US and European codes, a linear distribution is specified as a function of the normalized building height, while a bilinear distribution is employed in the New Zealand code. Severe earthquake damage to the nonstructural components in recent earthquakes and the resulting considerable economic losses led to concerns about the adequacy of the current code provisions. To evaluate the FAA distribution profile along the building height, recorded acceleration response of the instrumented buildings is analyzed using the California Strong Motion Instrumentation Program (CSMIP) database. FAA demand of three groups of buildings consisting of reinforced concrete, steel, and masonry buildings is analyzed. In each group, the buildings are classified into four subgroups according to the height. The mean FAA in the steel and reinforced concrete buildings are observed to be almost the same, while it is slightly smaller in the masonry buildings. The height of the structure is observed to affect the FAA, namely, the taller buildings generate larger FAA. The largest FAA generally appears at the top of the structure, where the magnitude varies from 3.0 to 8.0. Four levels of ground motions are considered in terms of the magnitude of peak ground acceleration (PGA), i.e., < 0.035 g, 0.035 – 0.1 g, 0.1 - 0.2 g, and > 0.2 g. Generally, smaller PGA generates larger FAA, e.g., in the concrete buildings, the corresponding FAAs are 3.55, 3.0, 2.11, and 1.55 for PGA < 0.035 g, 0.035 – 0.1 g, 0.1 - 0.2 g, and > 0.2 g, respectively, while they are slightly larger in steel buildings. Based on these observations, the inadequacies of the FAA distributions in current codes are highlighted. Using the CSMIP data and the simplified period calculation method suggested in ASCE 7-16, FAA distribution curves are developed for different period ranges. These new curves are expected to provide a better evaluation than that specified in ASCE 7-16.

Keywords: Floor acceleration; amplification; nonstructural component; seismic design; period

1. Introduction

Performance of structures in recent earthquakes have proven that the seismic design objectives can be achieved if the structural system is designed and constructed according to current seismic code provisions. However, damage to the nonstructural components (NCs) was frequently reported in recent major earthquakes with satisfactory structural performance (Gatscher et al., 2012; Goodno et al., 2011 [1,2]). Many types of NCs can be damaged in earthquakes and result in injuries and significant property losses (FEMA E-74 [3]). In general, the structural components of a commercial building account for approximately 15-25% of the original construction cost, while the NCs (mechanical, electrical, plumbing, and architectural) account for the remaining 75-85% of the cost (Whittaker and Soong, 2003 [4]). Therefore, reducing the earthquake damage of the NCs can significantly reduce the resulting economic losses. Based on their seismic response, there are three types of NCs, i.e., deformation, acceleration, and velocity sensitive (FEMA 273 [5]). In ASCE 7-16, some corresponding code provisions are provided to compute the deformation limit and the equivalent inertia force [6] for deformation and acceleration sensitive NCs. Equivalent inertia force represents the force experienced by the NCs during earthquake excitation and is widely used in the seismic design of NCs. Floor acceleration amplification (FAA) factor is one of the important parameters used in computing the equivalent seismic force. It represents the effect of the structure on amplifying the ground motion at the upper floors.

During the 17 January 1994 Northridge earthquake, a large amount of NCs were damaged or lost their function which caused considerable economic losses and increased the difficulty and duration of community recovery. After this earthquake, the seismic performance of the NCs, including the heightwise distribution profile of the FAA, was studied by many researchers. Drake and Gillengerten (1994) found that the magnitude of the peak floor acceleration increased with the floor levels in historical destructive earthquakes [7]. In an influential study, Drake and Bachman (1995) analyzed the roof acceleration responses of 150 buildings in California, which experienced 16 earthquakes between 1971 and 1994. A linear distribution profile of the FAA was developed and implemented in NEHRP 1994 [8-11]. Since then, the resulting linear distribution of FAA was accepted in the earthquake engineering community and widely used in the world. Recent studies based on nonlinear time history analysis of building structures explored the resulting heightwise FAA distributions using selected earthquake records. Miranda and Taghavi (2009) carried out analytical studies on buildings responding to earthquake ground motions in the elastic and inelastic range. Results indicate that the magnitude of FAA demand and its variation along the height are strongly dependent on the period of vibration, lateral resisting system and damping ratio of the building structure [12]. Taghavi and Miranda (2009) developed a response spectrum method to estimate FAA demand of multistory buildings considering the correlations between the modal accelerations and between the ground and modal accelerations [13]. Chaudhuri and Hutchinson (2011) performed nonlinear time history analysis of eight representative stiff and flexible steel moment resisting frames using 25 selected ground motions [14]. Codified profiles overestimate FAAs in nonlinear flexible frames with long fundamental periods, while underestimating the absolute floor accelerations at lower floor levels of stiff frames. The nonlinear behavior of the frames generally reduces FAA. Fathali and Lizundia (2011) developed a nonlinear distribution profile considering the fundamental vibration period of the main structure [15]. Pozzi and Kiureghian (2015) proposed a response spectrum analysis method based on the complete quadratic combination rule to estimate the peak floor acceleration (PFA). This method is able to provide a consistent estimation of the PFA along the entire structure [16]. Moschen et al. (2016) studied the prediction of the median PFA demand of elastic structures subjected to seismic excitation by means of an adapted response spectrum method using concepts of normal stationary random vibration theory [17]. Analytical studies of Anajafi and Medina (2018) indicate that the recommended FAA distribution profile in ASCE 7-16 does not envelope the recorded data in the instrumented buildings [18]. These studies offer some useful approaches to acquire reliable FAA for seismic evaluation of the NCs.

Although the studies in literature conclude that the actual FAA profile depends on several features of the main structure such as structural types, height, and soil site conditions, etc., and indicate that the current code provisions need to be visited, most of these studies are based on simulations with numerical models. In this study, floor acceleration response and FAA distribution profiles of the instrumented buildings in the California Strong Motion Instrumentation Program (CSMIP) are analyzed to develop a representative FAA distribution profile considering several parameters like structural types, height, etc. Developed profile is expected to be useful for the seismic deign of the NCs and applied in the future code provisions.

2. Current Code Provisions

Code provisions on the seismic design of the NCs have been issued in many countries in the world. Among the available codes, the most representative ones are ASCE 7-16, Eurocode 8, and New Zealand code 1170.5 ([6,19,20]). According to the ASCE 7-16 [6], the equivalent seismic design force of the NC is calculated as follows:

$$0.3S_{DS}I_pW_p \le F_p = \frac{0.4S_{DS}a_p}{R_p/I_p}\left(1+2\frac{z}{h}\right)W_p \le 1.6S_{DS}I_pW_p \quad (1)$$

where, F_p is the seismic design force applied at the center of gravity of the NC, I_p is the component importance factor, which takes a value of 1.0 or 1.5, W_p is the component operating weight, a_p is the component acceleration amplification factor, which varies from 1.0 to 2.5, the parameter $0.4S_{DS}$ corresponds to the factored mapped design spectral response acceleration at short periods, z is the elevation of the floor of the NC above grade, h is the elevation of the roof level above grade, and R_p is the component response modification factor. In the current version of the code, the relationship which involves the a_p term was simplified and replaced by a linear heightwise distribution, $(1+2z/h)$. It is 1.0 at the first floor and 3.0 at the roof level.

The Eurocode 8 [19] specifies a detailed design procedure for the seismic design of the NCs. The seismic analysis is based on a realistic model of the relevant structure and on the use of appropriate response spectra derived from the response of the main seismic resisting system. The effects of the seismic action can be determined by applying a horizontal force F_a to the NCs, which is defined as:

$$F_a = S_aW_a\gamma_a/q_a \quad (2)$$

where, F_a is the horizontal seismic force acting at the center of mass in the most unfavorable direction, W_a is the weight of the element, S_a is the seismic coefficient pertinent to NCs, γ_a is the importance factor where the importance of the NCs is assumed to have the same value as that of the main building, and q_a is the behavior factor, which is specified as 2.0 for the NCs. The seismic coefficient S_a can be calculated as:

$$S_a = \alpha S\left[\frac{3(1+z/H)}{1+(1-T_a/T_1)^2}-0.5\right], \quad \alpha = a_g/g \quad (3)$$

where, a_g is the design ground acceleration, g is the acceleration of gravity, S is the soil factor, T_a is the fundamental period of the NC, T_1 is the fundamental vibration period of the building in the relevant direction, z is the elevation of the floor of the NC with respect to the level of the application of the ground motion (normally the ground level), and H is the height of the building. From Eq. (3), one can find that the magnitude of FAA at the roof level is 2.0, which is smaller than the one specified in ASCE 7-16 [6]. On the other hand, Eq. (3) takes into account the fundamental periods of the main building and the NCs. T_1 can be obtained using an approximate method, while there is no immediate available method to compute T_a. Therefore, practical application of Eq. (3) is questionable.

In the New Zealand seismic design code [20], the design response coefficient $C_p(T_p)$ for a NC supported at level i of a structure is the horizontal acceleration coefficient computed at the level of structure that provides support for the NC. It is determined as follows:

$$C_p(T_p) = C(0)C_{Hi}C_i(T_p) \quad (4)$$

where $C(0)$ is the site hazard coefficient for $T = 0$, corresponding to the peak ground acceleration, C_{Hi} is the floor height coefficient for level i, T_p is the period of the NC, and $C_i(T_p)$ is the NC's spectral shape factor at level i. The floor acceleration coefficient at level i, C_{Hi}, is calculated from Eq. (5), (6), or (7), as appropriate for the elevation of the support floor of the NC. For elevations that satisfy the height limitations of more than one condition listed below, the lesser value of C_{Hi} is used.

$$C_{Hi} = 1 + h_i/6 \qquad \text{for } h_i < 12\text{m} \tag{5}$$
$$C_{Hi} = 1 + 10h_i/h_n \qquad \text{for } h_i < 0.2h_n \tag{6}$$
$$C_{Hi} = 3.0 \qquad \text{for } h_i \geq 0.2h_n \tag{7}$$

where h_i is the elevation of the story level of the NC, and h_n is the distance between the base of the structure and the uppermost seismic weight or mass. C_{Hi} for levels below ground floor level is taken the same as ground floor level. The spectral shape coefficient, $C_i(T_p)$, is the ordinate of the tri-linear spectral acceleration function corresponding to T_p. Ordinates of the spectral shape factor of the NC are given as follows:

$$\begin{aligned} C_i(T_p) &= 2.0 && \text{for } T_p \leq 0.75s \\ &= 0.5 && \text{for } T_p \geq 1.5s \\ &= 2(1.75 - T_p) && \text{for } 0.75s < T_p < 1.5s \end{aligned} \tag{8}$$

From Eqs. (5) to (8), one can observe that New Zealand code suggests the identical heightwise distribution of the FAA with Eurocode 8. However, a different method taking into account of the fundamental period of the NC is given in this code.

Almost all the current code provisions on the FAA employ the linear or bilinear distribution profile using the normalized elevation (*z*/*h*) as a parameter. The FAA profiles specified by different code provisions are plotted in Fig. 1. From this figure, it is observed that FAAs used in the earlier version of the codes were conservative. The largest FAA is 4.0 in NEHRP 1994 and UBC 1997. Then, based on extensive amount of analytical work conducted, the magnitude of FAA is reduced in the recent code provisions such as ASCE 7-16, Eurocode 8, [6,19] etc. In the current codes, the general suggested value for FAA is 3.0 at the roof level. It is noted that almost all the suggested FAAs are based on the pioneer analytical studies of Drake and Bachman [8,9] where the recorded floor acceleration responses in the instrumented buildings were processed in a statistical approach. The structural types and fundamental vibration period are not considered, therefore the FAA profiles developed as a result of this study may not be fully representative. Accordingly, it is necessary to reanalyze these recorded data, and many others measured after this study, considering these two parameters.

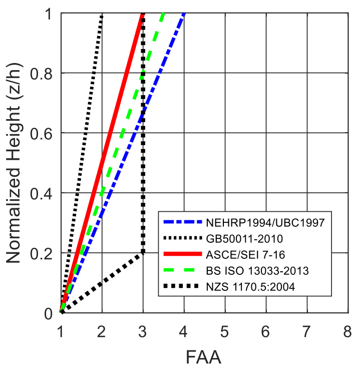

Fig. 1. FAA in current code provisions

3. Analysis Method

3.1 Building Height Classification

The influence of the building height on the magnitude of FAA is not considered in the current code provisions because elevation of the NCs (*z*) is normalized by the overall height of the building (*h*). Previous studies have been proved that the largest magnitude of the FAA in a building often appears at the roof level [8,9]. In addition, as a result of the whiplash effect, tall buildings can generate rather larger FAAs compared to low-rise buildings under the same earthquake excitation [21]. Consequently, the height of the building should be classified before processing the distribution profile of the FAA along the normalized height (*z*/*h*).Regarding the number of stories, according to the classification adopted in the CSMIP database, buildings can be categorized as low-rise (1-6 stories), mid-rise (7 to 12 stories), and high-rise (more than 13stories).Preliminary analytical results show that the magnitudes of the FAA are almost the same in the buildings from 1 to 13 stories and it is difficult to find a consistent trend to describe the heightwise distribution profile. Furthermore, modern building design and construction technologies have been developed significantly in the past two decades. Accordingly, a more qualified classification method than the current one adopted in the CSMIP database is needed. For example, in Fathali and Lizundia (2011) [15], number of stories larger than 15 was regarded as one category. This method sounds reasonable but needs further extensive statistical analysis of the height of the existing buildings. Based on the data mining analysis of the building heights worldwide, a new height classification standard was proposed by emporis company [www.emporis.com] and shown in Table 1. According to this classification, the category of the mid-rise was removed from the traditional standard mentioned above and the new categories of skyscraper, supertall, and megatall were added. In the new standard, the corresponding height levels are 0 to 35 m, 35 to 100 m, 100 to 300 m, 300 to 600 m, and larger than 600 m, for the low-rise, high-rise, skyscraper, supertall, and megatall buildings, respectively. This standard is followed in processing the FAA distribution profiles in the instrumented buildings with various height levels.

Besides the height standard, the height limit of the building is determined by its structural type. In many codes for seismic design of building structures, a height limit is usually recommended for each structural type. Accordingly, a structural type classification in terms of the building materials is applied. The resulting categories are concrete, steel, and masonry buildings.

Table 1. Building height classification

Classification	Height (m)	Story
Lowrise	≤ 35	< 12
Highrise	35 – 100	12 -39
Skyscraper	100 - 300	> 40
Supertall	300 – 600	--
Megatall	> 600	--

Table 2. Amount of buildings and earthquakes

Building Type	Height Level	# Building	Earthquake Record			
			PGA<0.035	0.035g<PGA<0.1g	0.1g<PGA<0.2g	PGA>0.2g
Concrete	Low-rise	49	224	55	15	10
	High-rise	21	85	27	7	5
	Skyscraper	2	5	--	--	--
Steel	Low-rise	57	237	44	9	6
	High-rise	34	113	17	7	--
	Skyscraper	5	19	5	1	--
Masonry	Low-rise	15	82	19	5	2
Total		183	765	167	44	23

3.2 Earthquake Records

In the CSMIP database, there are totally 183 buildings consists of 72 concrete buildings, 96 steel buildings, and 15 masonry buildings. The number of the earthquake records of interest is 999. To distinguish the magnitude of the peak ground accelerations (PGAs), the earthquake intensity level is classified in terms of PGA according to the seismic design code of China [22],where the PGAs are 0.035, 0.1, and 0.2 g, for the frequent, basic, and rare earthquakes (Table 2). Accordingly, there are four earthquake groups and the corresponding amount of the records are 765, 167, 44, and 23 (Table 2). There are 178 buildings lower than 300 m, which is about 97.3% of the total amount of the buildings. Most of the PGAs of the earthquake records are smaller than 0.1 g and the corresponding amount of the records is 932, which is about 93.2% of the total records. On account of the social and economic development levels, there are no records on the supertall and megatall buildings. Most of the masonry buildings are lowrise. Therefore, for the FAAs in the supertall and megatall buildings, specific floor acceleration response analysis is required to obtain qualified heightwise distribution profiles [23].

3.3 Regression Method

The linear distribution profile of the FAA can envelop a considerable amount of the measured data points along the building height. Linear profile achieves the maximum value at the roof level which is consistent with the data measured in most instrumented buildings. However, in the stories near the ground and other levels, there are still many data points that are not enveloped by the linear profile in the code provisions, therefore it is necessary to develop a more reliable profile to represent the fundamental dynamic properties and envelop most of the recorded FAA data. Statistical studies have been carried out in literature for this purpose [14,15,24]. Fathali and Lizundia (2012) suggested a nonlinear distribution profile based on regression analysis as shown below:

$$FAA = 1 + \alpha\left(z / h\right)^{\beta} \tag{9}$$

where, α is a velocity factor to determine the heightwise incremental velocity of the profile, and β is a shape factor for determining the geometric shape of the profile. When $\alpha = 2.0$ and $\beta = 1.0$, Eq. (9) becomes identical to the profile suggested in ASCE 7-16 ([6]). In fact, the shape factor, β, has a function of enveloping the data points. More FAA data are enveloped with increasing magnitude of β. When $\beta > 1.0$, the resulting FAA will envelop smaller amount of the data points in the lower stories of the building, therefore $\beta < 1.0$ is preferred to envelop more data, where parametric analysis indicates that $\beta = 0.5$ is a good estimation. The resulting distribution profile is a parabola. The other factor (α) can be acquired through regression analysis. Resulting FAA is represented with Eq. (10) and explored in more detail in the next section as it is an appropriate improvement to the linear code profile

$$FAA = 1 + \alpha\left(z / h\right)^{0.5} \tag{10}$$

4. FAA Distribution Profile

4.1 Concrete Buildings

The height distribution of the concrete buildings is shown in Fig. 2. From this figure, one can observe that most of the instrumented concrete buildings are low-rise, which is about 68.1% of the total amount of the buildings. In addition to the low-rise buildings, there are 21 high-rise, and 2 skyscraper buildings. The FAA data and the profile according to Eq. (10) are plotted in Fig. 3. From this figure, it is observed that the magnitude of PGA does not strictly affect the FAA profile. Compared to the ASCE 7-16 [6], more data points (more than 80%) are enveloped in the range of $z/h < 0.35$. However, the peak values of FAA at the roof levels are smaller than those provided in ASCE 7-16 [6]. For the skyscrapers, the resulting FAA profiles regressed from limited records are close to those in ASCE 7-16 [6]. The related parameters on the results of the regressing process are shown in Table 3. From this table, one can observe that: 1) in the low-rise buildings, the magnitude of PGA has slight influence on the velocity factor, α, until PGA=0.2g, above which it increases significantly. 2) Overall, α is larger for the high-rise buildings compared to the low-rise buildings. The peak value of α corresponds to PGA between 0.1 to 0.2 g, while for PGA > 0.2 g, α decreases to the level corresponding to PGA < 0.035 g. 3) For the skyscraper buildings, only the FAA data in the earthquakes with PGA < 0.035 g are obtained. The corresponding α value is the largest (1.45).

At the roof level, most of the obtained FAA are beyond the regressed profiles (Fig. 3). This trend reduces the applicability of the suggested FAA. To explore this issue further, all mean FAA values of the roof levels for every earthquake group were computed and shown in Table 3 and plotted in Fig. 4 together with the corresponding standard deviations. One can observe that: 1) The magnitude of the FAA decreases with the building height in all earthquake groups. 2) For buildings with the same height, FAA decreases with increasing PGA. 3) In the low earthquake excitation (PGA < 0.1 g), most of the FAAs in the high-rise buildings are larger than 3.0, which is the value provided in ASCE 7-16 [6], while the FAAs in low-rise buildings are all larger than 3.0 at any earthquake level. In the supertall buildings, due to the strong whiplash effect, the resulting FAA near the roof is very large [24]. Comprehensive floor response analysis is needed to obtain a reliable FAA parameter.

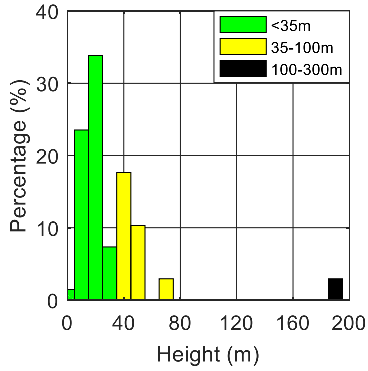

Fig. 2. Height distribution of the concrete buildings

Table 3. Parameters of FAA in concrete buildings

Height Type	PGA (g)	α	Roof Mean (μ)	Standard Deviation (σ)
Low-rise (0-35m)	<0.035	1.24	3.67	0.19
	0.035-0.1	1.26	3.42	0.36
	0.1-0.2	1.27	3.10	0.67
	>0.2	1.39	2.68	0.41
High-rise (35-100m)	<0.035	1.35	3.56	0.36
	0.035-0.1	1.37	3.00	0.53
	0.1-0.2	1.41	2.11	0.67
	>0.2	1.35	1.55	0.49
Skyscraper (100-300m)	<0.035	1.45	3.63	1.87
	0.035-0.1	--	--	--
	0.1-0.2	--	--	--
	>0.2	--	--	--

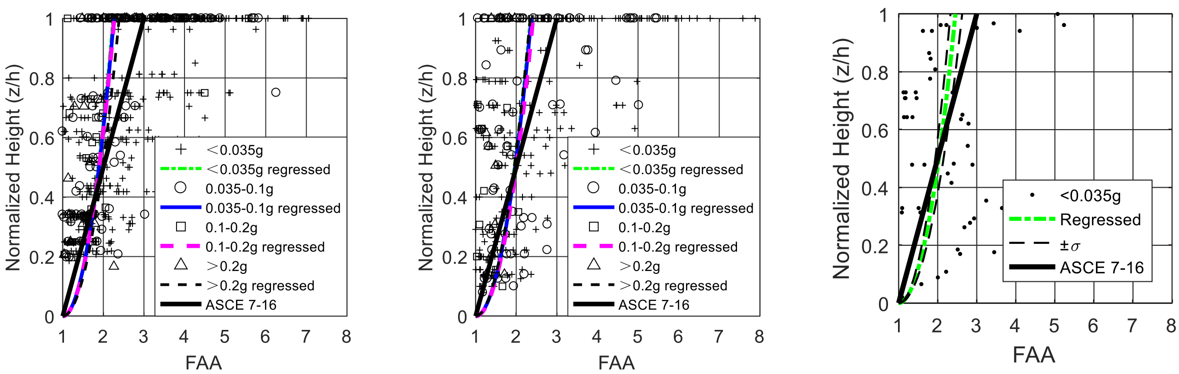

a). Lowrise b). Highrise c). Skyscraper (PGA < 0.035 g)

Fig. 3. Regressed FAA distributions in concrete buildings

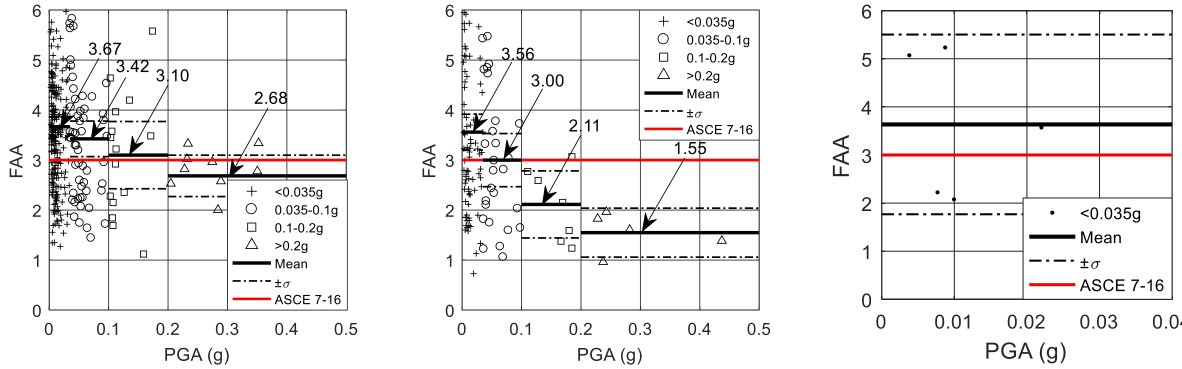

a). Lowrise b). Highrise c). Skyscraper (PGA < 0.035 g)

Fig. 4. FAA at the roof of concrete buildings

4.2 Steel Buildings

There are 57 low-rise, 34 high-rise, and 5 skyscraper steel buildings. As shown in Fig. 5, the height of the steel buildings is generally taller than those of the concrete buildings. The regressed FAA profiles have a trend similar to those of the concrete buildings. At the height level of $z/h > 0.8$, the FAA in the earthquakes of PGA > 0.1 g is larger than that of the PGA < 0.1 g. The mean FAA in the roof of all the buildings are listed in Table 4 and plotted in Fig. 7. In the PGA range between 0.035 and 0.1 g, the resulting FAAs are smaller than those of the concrete buildings. The magnitude of α increases with increasing PGA and building height. It is smaller than 1.44 in the low-rise, and 1.47, 1.49 in the high-rise and skyscraper buildings. Level of FAA reduces with the increasing PGA. The largest mean FAA appears in the low-rise buildings (3.69), and smallest one appears in the skyscraper buildings (3.06). The largest measured FAA is about 8.0.

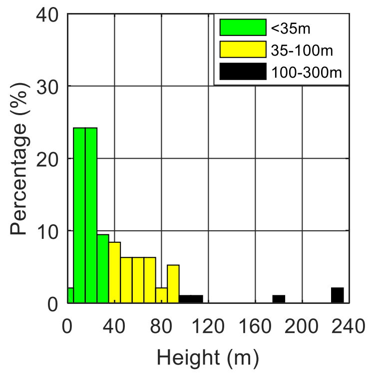

Fig. 5. Height percentage of the steel buildings

Table 4. Parameters on FAA in steel buildings

Height Type	PGA (g)	α	Roof Mean (μ)	Standard Deviation (σ)
Low-rise (0-35m)	<0.035	1.26	3.69	0.23
	0.035-0.1	1.24	2.80	0.44
	0.1-0.2	1.33	3.02	0.99
	>0.2	1.44	2.17	0.69
High-rise (35-100m)	<0.035	1.28	3.27	0.39
	0.035-0.1	1.30	2.18	0.80
	0.1-0.2	1.47	1.99	0.81
	>0.2	-	-	-
Skyscraper (100-300m)	<0.035	1.41	3.06	0.70
	0.035-0.1	1.37	2.68	1.70
	0.1-0.2	1.49	2.88	-
	>0.2	-	-	-

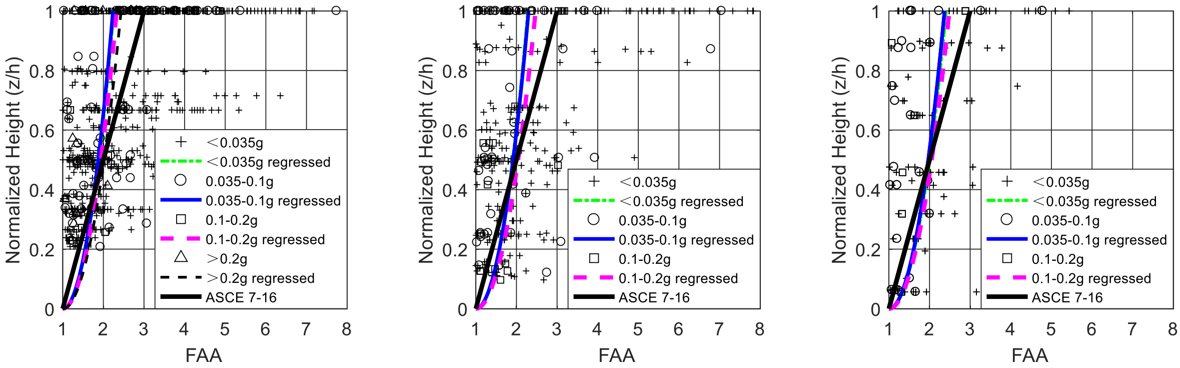

a). Lowrise b). Highrise c). Skyscraper (PGA < 0.035 g)

Fig. 6. Regressed FAA distributions in steel buildings

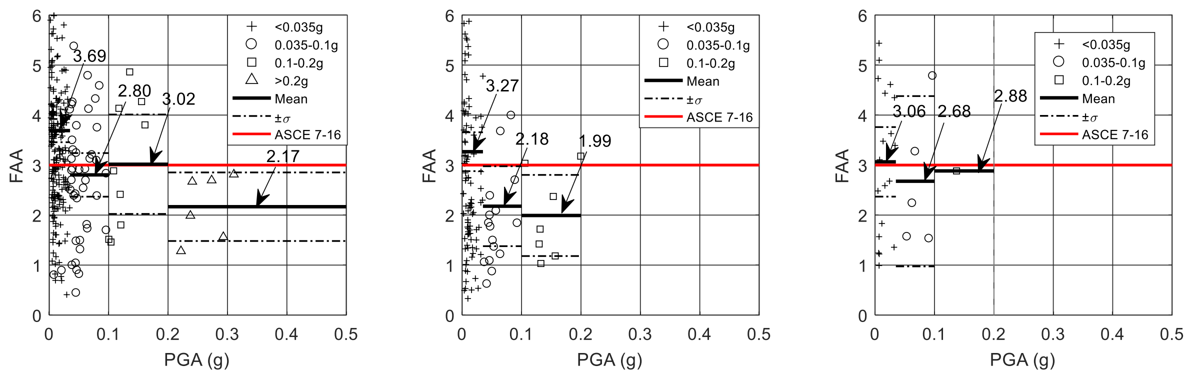

a). Lowrise b). Highrise c). Skyscraper (PGA < 0.035 g)

Fig. 7. FAA at the roof of the steel buildings

4.3 Masonry Buildings

There are 15 masonry buildings and all of them are lower than 35 m (Fig. 8). Limited earthquake records in the CSMIP database are analyzed. Almost all the obtained FAA values are smaller than 3.0 except the ones at the roof levels (Fig. 9). Most of the data points are located between 0.3 and 0.5 *z/h*. The value of α value increases with the PGA. Similar to the concrete and steel buildings, the FAA at the roof is obviously larger than the other locations. The largest mean FAA is 3.90 corresponding to PGA levels between 0.1 and 0.2 g. The actual maximum FAA is about 7.0 (Fig. 10).

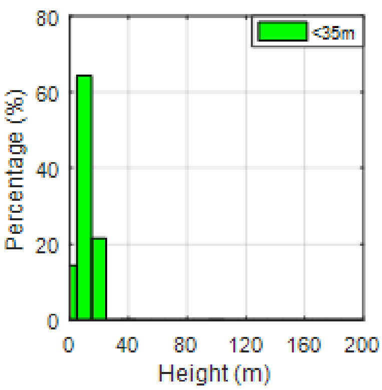

Fig. 8. Height percentage of the masonry buildings

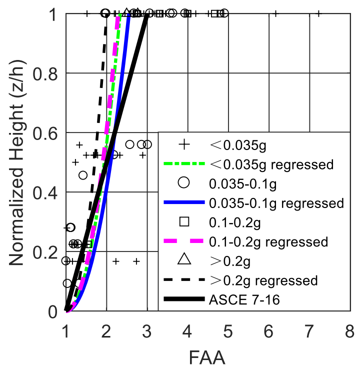

Fig. 9. Regressed FAA distributions in masonry buildings

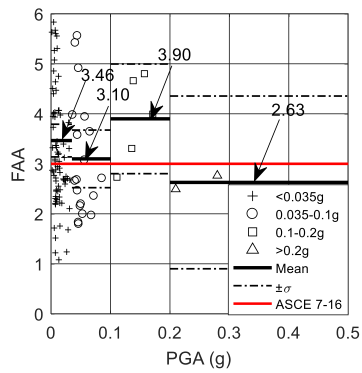

Fig. 10. FAA in the roof of the masonry buildings

5. Discussion

5.1 Velocity Factor and FAA at the Roof

Based on the regressed velocity factors (α) in the previous sections, a group of suggested values at the roof level for each building type are listed in Table 5. As indicated in the previous section, the FAA values decrease with building height and with increased PGA. FAA values of concrete and masonry buildings are consistently larger than those of steel buildings, although there is not a significant difference in the values. The recommended FAA values for the tall buildings are conservative and further data are needed to make the estimation reliable enough.

Table 5. Suggested α and FAA in the roof for different building types

Height	**PGA (g)**	**α**			**FAA**		
		Concrete	**Steel**	**Masonry**	**Concrete**	**Steel**	**Masonry**
Lowrise (0-35 m)	< 0.035	1.30	1.35	1.60	3.80	3.80	3.50
	0.035-0.1	1.30	1.35	1.60	3.50	3.00	3.20
	0.1-0.2	1.30	1.35	1.35	3.20	3.10	4.00
	> 0.2	1.40	1.45	1.10	2.70	2.20	2.70
Highrise (35-100 m)	< 0.035	1.40	1.35	--	3.60	3.30	--
	0.035-0.1	1.40	1.35	--	3.00	2.20	--
	0.1-0.2	1.45	1.50	--	2.10	2.00	--
	> 0.2	1.40	1.45	--	1.60	1.50	--
Skyscraper (100-300 m)	< 0.035	1.50	1.45	--	3.70	3.10	--
	0.035-0.1	1.45	1.40	--	3.60	3.00	--
	0.1-0.2	1.55	1.50	--	2.00	2.90	--
	> 0.2	1.50	1.45	--	1.50	2.50	--

Table 6. Fundamental period range

Height Level	Height Range (m)	Period (sec)		
		Concrete	Steel	Masonry
Lowrise	≤ 35	≤ 1.1	< 1.2	< 0.7
Highrise	35-100	1.1-2.5.	1.2-2.7.	0.7-1.6.
Skyscraper	100-300	2.4-5.4	2.7-6.1	1.6-3.6
Supertall	300-600	5.4-9.1	6.1-10.3	3.6-6.1
Megatall	> 600	> 9.1	> 10.3	> 6.1

5.2 Influence of the Vibration Period

To consider the effect of the fundamental vibration period of the main building, the simplified method in ASCE 7-16 [6], Eq. 11, is adopted

$$T=C_t H^{3/4} \tag{11}$$

where, T is the fundamental vibration period of the building and C_t is a coefficient related to the structural type. The corresponding values of C_t for the concrete, steel, and masonry buildings are 0.075, 0.085, and 0.05, respectively. The period ranges of the buildings in the CSMIP database are listed in Table 6. With these period range, the FAA distribution profile can be divided into three groups: namely $T < 0.5$ sec, $0.5 \leq T < 1.5$ sec, and $T \geq 1.5$ sec. The FAA profiles in these period ranges obtained from the Fathali and Lizundia (2011) [15] equation are plotted in Fig. 11 along with the ASCE7-16 [6] equation. It can be observed from this figure that the suggested distribution profile for the lowrise steel buildings (solid black line) is much more reasonable that that given in Fathali and Lizundia (2011) as it envelops more data points shown in Fig. 3, Fig. 6 and Fig. 9.

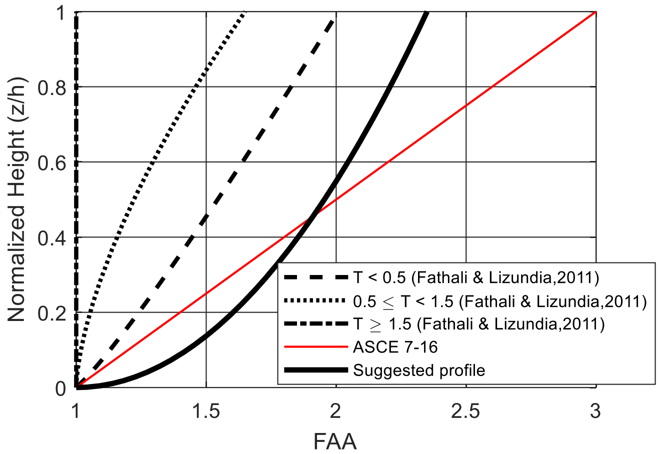

Fig. 11. FAA distribution considering vibration period

6. Conclusions

The seismic performance of non-structural components attracted significant attention in the earthquake engineering community. The Floor Acceleration Amplification (FAA) is one of the critical parameters in computing the equivalent seismic force of the NCs. In this study, FAAs in the instrumented buildings of the CSMIP database are processed considering their structural types, heights, and fundamental vibration periods. Some conclusions are addressed below:

1) The height of the buildings is classified using a new categorization consisting of 5 height levels. i.e. low-rise, high-rise, supertall, and megatall.
2) Parabolic distribution profiles are suggested which can envelop most of the FAA data as demonstrated by the processed results. The velocity factor proposed in Fathali and Lizundia [15] is employed to represent the increment velocity of the parabola.
3) The obtained FAAs at the roof is generally larger than those in other levels. A group of specific values are recommended considering this observation.
4) The vibration period of the building influences the magnitude of the FAA, and this effect is taken into account by classifying the buildings according to period ranges. In future studies, it is recommended to employ the building period in the FAA equations
5) For the supertall and special buildings, a comprehensive floor acceleration response analysis is needed to acquire a reliable FAA distribution.

Acknowledgements

The presented research is funded by China National Science and Technology Major Project with grants # 2018YFC0705701, and China National Science Foundation with grants # 51608381, 51578405.

References

[1] Gatscher JA, McGavin GL, Caldwell PJ (2012). Earthquake Protection of Building Equipment and Systems, Bridging the Implementation Gap, ASCE, Reston, Virginia, USA.

[2] Goodno BJ, Gould NC, Caldwell PJ, and Gould PL (2011). Effects of the January 2010 Hatian Earthquake on Selected Electrical Equipment. *Earthquake Spectra*, **27**(S1): 1-26.
[3] Federal Emergency Management Agency (FEMA) (2012). *Reducing the Risks of Nonstructural Earthquake Damage – A Practical Guide.* FEMA E-74, Federal Emergency Management Agency, Washington, USA.
[4] Whittaker AS. and Soong TT (2003). An overview of nonstructural component research at three U.S. earthquake engineering research centers. *Proceedings of Seminar on Seismic Design, Performance, and Retrofit of Nonstructural Components in Critical* Facilities, Applied Technology Council, ATC-29-2, Redwood City, California, pp. 271-280.
[5] Federal Emergency Management Agency (FEMA) (1997). *NEHRP Guidelines for the Seismic Rehabilitation of Buildings*. FEMA 273, Federal Emergency Management Agency, Washington, USA.
[6] American Society of Civil Engineers (ASCE). (2017). *Minimum Design Loads for Buildings and Other Structures. ASCE/SEI 7-16*, American Society of Civil Engineers: Reston, VA, USA.
[7] Drake RM, Gillengerten JD (1994). Examination of CDMG Ground Motion Data in Support of the 1994 NEHRP Provisions. *Proc. 5th U.S. National Conference on Earthquake Engineering*. Earthquake Engineering Research Institute, Chicago, Ill, pp. 745-754.
[8] Drake R, Bachman R (1995). Interpretation of instrumented building seismic data and implications for building codes. *Proc. the 64th Annual Convention of the Structural Engineers Association of California*, Structural Engineers Association of California, Indian Wells, CA, October 19-21.
[9] Drake R, Bachman R (1996). NEHRP provisions for 1994 for nonstructural components. *Journal of Architectural Engineering*, **2**(1): 26-31.
[10] Soong TT, Bachman RE, and Drake RM. Implication of 1994 Northridge earthquake on design guidelines for nonstructural components. *Proc. the NEHRP conference and workshop on research on the Northridge*, California earthquake of January 17, 1994, Richmond, CA, 1998.
[11] Building Seismic Safety Council (BSSC) (1994, 1997, 2000, 2003). *NEHRP recommended provisions for the development of seismic regulations for new buildings and other structures*. National Earthquake Hazards Reduction Program, Washington, DC.
[12] Miranda E, Taghavi S (2005). Approximate Floor Acceleration Demands in Multistory Buildings I: Formulation. *Journal of Structural Engineering*, **131**(2): 203-211.
[13] Taghavi S, Miranda E (2005). Approximate Floor Acceleration Demands in Multistory Buildings II: Applications. *Journal of Structural Engineering*, **131(**2): 212-220.
[14] Chaudhuri SR., and Hutchinson TC (2011). Effect of nonlinearity of frame buildings on peak horizontal floor acceleration. *Journal of Earthquake Engineering*, **15**(1): 124-142.
[15] Fathali S, and Lizundia B (2011). Evaluation of current seismic design equations for nonstructural components in tall buildings using strong motion records. *The Structural Design of Tall and Special Buildings*, **20**(S1): 30-46.
[16] Pozzi M., and Kiureghian AD (2015). Response spectrum analysis for floor acceleration. *Earthquake Engineering and Structural Dynamics*, **44**(12): 2111-2127.
[17] Moschen L, Adam C, Vamvatsikos D (2016). A response spectrum method for peak floor acceleration demands in earthquake excited structures. *Probabilistic Engineering Mechanics*, **46**:94-106.
[18] Anajafi H, and Medina R (2018). Evaluation of ASCE 7 equations for designing acceleration sensitive nonstructural components using data from instrumented buildings. *Earthquake Engineering and Structural Dynamics*, **47**(4): 1075-1094.
[19] European Committee for Standardization (2005). *Eurocode 8: Design of Structures for Earthquake Resistance- Part 1: General Rules, Seismic Actions and Rules for Buildings*. BS EN 1998-1:2004, Brussels.
[20] Standards New Zealand (2004). *Structural Design Actions, Part 5: Earthquake Actions*. NZS 1170.5, Wellington, New Zealand.
[21] Lu W, Huang B, Mosalam KM, and Chen S. (2016). Experimental evaluation of a glass curtain wall of a tall building. *Earthquake Engineering and Structural Dynamics*, **45**(7), 1185-1205.
[22] Ministry of Housing and Urban-Rural Development of the People's Republic of China (MOUHRD) (2016). *Code for Seismic Design of Buildings*. GB50011-2010, Building Industry Press of China, Beijing, China. (in Chinese)
[23] Lu W, Huang W, Chen S, and Mosalam KM (2017). Acceleration Demand of the Outer-skin Curtain Wall System of the Shanghai Tower. *The Structural Design of Tall and Special Buildings*, **26**(5): DOI: 10.1002/tal.1341.
[24] Huang B, Lu W, and Cao W (2009). Discussion on the seismic performance indices of architectural curtain wall. *China Civil Engineering Journal*, **42**(9): 7-12. (in Chinese)

